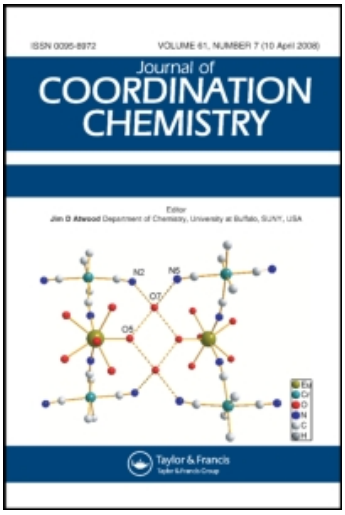

Journal of Coordination Chemistry
Publication details, including instructions for authors and subscription information:
http://www.informaworld.com/smpp/title~content=t713455674

Synthesis, structures and properties of ternary rare earth complexes with fluorobenzoic acid and 1,10-phenanthroline

Li-Juan Xu[a]; Shu-Ping Wang[a]; Rui-Fen Wang[a]; Jian-Jun Zhang[b]
[a] Department of Chemistry, Hebei Normal University, Shijiazhuang 050016, P.R. China [b] Experimental Center, Hebei Normal University, Shijiazhuang 050016, P.R. China

First published on: 22 September 2010

To cite this Article Xu, Li-Juan , Wang, Shu-Ping , Wang, Rui-Fen and Zhang, Jian-Jun(2008) 'Synthesis, structures and properties of ternary rare earth complexes with fluorobenzoic acid and 1,10-phenanthroline', Journal of Coordination Chemistry, 61: 2, 237 — 250, First published on: 22 September 2010 (iFirst)
To link to this Article: DOI: 10.1080/00958970701324036
URL: http://dx.doi.org/10.1080/00958970701324036

Journal of Coordination Chemistry
Vol. 61, No. 2, 20 January 2008, 237–250

Taylor & Francis
Taylor & Francis Group

Synthesis, structures and properties of ternary rare earth complexes with fluorobenzoic acid and 1,10-phenanthroline

LI-JUAN XU†, SHU-PING WANG†, RUI-FEN WANG*†
and JIAN-JUN ZHANG‡

†Department of Chemistry, Hebei Normal University, Shijiazhuang 050016, P.R. China
‡Experimental Center, Hebei Normal University, Shijiazhuang 050016, P.R. China

(*Received 21 October 2006; revised 9 December 2006; in final form 12 December 2006*)

Three dimeric rare-earth complexes $[Eu(p\text{-}FBA)_3(phen)(H_2O)]_2$ (**1**), $[Tb(p\text{-}FBA)_3phen]_2$ (**2**), and $[Tb(o\text{-}FBA)_3phen]_2$ (**3**) (where p-FBA = p-fluorobenzoate, o-FBA = o-fluorobenzoate, phen = 1,10-phenanthroline) were synthesized and structurally characterized. All are neutral dimeric molecules. Complex **1** crystallizes in triclinic system, space group $P\bar{1}$. Each Eu(III) ion is eight-coordinate with one 1,10-phenanthroline, one monodentate carboxylate, one water and four bridging carboxylates. Complex **2** crystallizes in triclinic system, space group $P\bar{1}$. Each Tb(III) is also eight-coordinate with one 1,10-phenanthroline molecule, one bidentate chelating carboxylate and four bridging carboxylates. Complex **3** crystallizes in the monoclinic system, space group $P2_1/c$ and consists of two crystallographically different binuclear molecules. Tb(III) ions are eight-coordinate with one 1,10-phenanthroline, one bidentate chelating carboxylate and four bridging carboxylates in both of them. Complex **1** shows bright red luminescence, **2** and **3** show green luminescence under UV light at room temperature. Thermal analysis indicates that are all quite stable to heat.

Keywords: Terbium complex; Europium complex; Crystal structure; Luminescence; Fluorobenzoic acid; 1,10-Phenanthroline

1. Introduction

Structures of rare-earth carboxylate complexes are diverse due to the high coordination number of central ions (usually eight or nine), and the various coordination modes of carboxylate groups (such as chelating bidentate, bridging bidentate and bridging tridentate) [1–16]. These complexes are stable in air, leading to intensive study for new rare-earth fluorescent materials, electroluminescent materials and potential applications of luminescent probes [17–19]. The luminescent properties of such complexes were closely related to their composition and structures, such as the nature of organic ligands, even different substituents on the ligands, and the coordination environment of central ions [20–29]. In previous work, we found that neutral conjugated heterocyclic ligands (such as phen or bipy) can enhance the luminescent intensity in Eu(III) or Tb(III) carboxylate compounds. In studies about rare-earth aromatic carboxylate

*Corresponding author. Email: wruifen@mail.hebtu.edu.cn

Journal of Coordination Chemistry
ISSN 0095-8972 print/ISSN 1029-0389 online © 2008 Taylor & Francis
DOI: 10.1080/00958970701324036

complexes, chlorobenzoic acids and bromobenzoic acids have been used as ligands [26, 29, 30], but the fluorobenzoic acids have seldom been used. In order to compare the properties of complexes in this series, we synthesized three ternary rare-earth complexes of fluorobenzoic acids with 1,10-phenanthroline: [Eu(*p*-FBA)$_3$(phen)(H$_2$O)]$_2$ (**1**), [Tb(*p*-FBA)$_3$phen]$_2$ (**2**) and [Tb(*o*-FBA)$_3$phen]$_2$ (**3**). Their crystal structures, luminescent properties and thermal analysis are reported in this article.

2. Experimental

2.1. *General*

All chemicals were analytical grade. $EuCl_3 \cdot 6H_2O$ and $TbCl_3 \cdot 6H_2O$ were prepared by dissolving their oxides in hydrochloric acid, and then drying the solution by water-bath heating. Elemental analysis was carried out on a Flash EA 1112 elemental analyzer. The fluorescence properties of powder samples were determined using a Hitachi F-4500 fluorescence spectrophotometer at room temperature. TG and DTG experiments were performed using a Perkin-Elmer TGA7 thermogravimetric analyzer at heating rate $10^\circ C\,min^{-1}$ in nitrogen. The IR spectra were taken on a FT-IR spectrometer using KBr pellets.

2.2. *Preparation of complexes*

Stoichiometric amounts of $EuCl_3 \cdot 6H_2O$, *p*-fluorobenzoic acid and 1,10-phenanthroline were dissolved separately in 95% C_2H_5OH. The pH of the *p*-fluorobenzoic acid solution was adjusted in a range of 6–7 with 1 M NaOH solution. The C_2H_5OH solutions of the ligands were mixed and then the mixture was added dropwise to the ethanolic $EuCl_3$ solution under stirring, while a white precipitate formed. The solution was stirred for 4 h at room temperature and filtered. Colorless transparent crystals suitable for X-ray analysis were obtained by slow evaporation of the filtrates. Calcd for **1**, $C_{66}H_{44}N_4O_{14}F_6Eu_2$ (%): C, 51.64; H, 2.89; N, 3.65. Found: C, 52.08; H, 2.58; N, 3.97.

The synthesis of **2** is similar to that of **1**, whereas $TbCl_3 \cdot 6H_2O$ was used instead of $EuCl_3 \cdot 6H_2O$. Calcd for **2**, $C_{66}H_{40}N_4O_{12}F_6Tb_2$ (%): C, 52.40; H, 2.66; N, 3.70. Found: C, 52.17; H, 2.28; N, 3.97.

The synthesis of **3** is similar to that of **2**, but *o*-fluorobenzoic acid was used instead of *p*-fluorobenzoic acid. Calcd for **3**, $C_{66}H_{40}N_4O_{12}F_6Tb_2$ (%): C, 52.40; H, 2.66; N, 3.70. Found: C, 52.03; H, 2.25; N, 3.97.

2.3. *X-ray crystallography*

X-ray crystallographic data collections for the complexes were carried out on a Bruker SMART APEX II CCD area detector equipped with a graphite-monochromated Mo-Kα radiation ($\lambda = 0.71073$ Å) at 293(2) K. Semi-empirical absorption corrections were applied by the SADABS program. The structures were solved by direct methods with SHELXS-97 [31] and refined using a full-matrix least-squares procedure on F^2 in SHELXL-97 [32]. Hydrogen atoms were added theoretically and refined with riding model position parameters and fixed isotropic thermal parameters.

Table 1. Crystal structure data for **1**, **2** and **3**.

Compound	**1**	**2**	**3**
Empirical formula	$C_{33}H_{22}F_3N_2O_7Eu$	$C_{66}H_{40}F_6N_4O_{12}Tb_2$	$C_{66}H_{40}F_6N_4O_{12}Tb_2$
Formula weight	767.49	1512.86	1512.86
Temperature (K)	293(2)	293(2)	293(2)
Wavelength (Å)	0.71073	0.71073	0.71073
Crystal system	Triclinic	Triclinic	Monoclinic
Space group	$P\bar{1}$	$P\bar{1}$	$P2_1/c$
Unit cell dimensions (Å, °)			
a	8.3682(7)	9.888(1)	19.918(1)
b	12.758(1)	11.774(1)	15.154(1)
c	14.922(1)	14.765(2)	20.566(1)
α	96.731(1)	111.906(1)	90
β	103.054(1)	101.523(1)	109.859(1)
γ	98.789(1)	101.583(1)	90
Volume (Å^3), Z	1514.5(2), 2	1489.3(3), 1	5838.3(7), 4
Calculated density (g cm^{-3})	1.683	1.687	1.721
Absorption coefficient (mm^{-1})	2.141	2.442	2.491
$F(000)$	760	744	2976
Crystal size (mm^3)	0.22 × 0.16 × 0.14	0.22 × 0.20 × 0.16	0.22 × 0.20 × 0.16
θ range for data collection (°)	2.33 to25.03	1.91 to 25.03	1.73 to 25.03
Limiting indices	$-9 \le h \le 9$, $-15 \le k \le 15$, $-17 \le l \le 17$	$-11 \le h \le 10$, $-13 \le k \le 14$, $-14 \le l \le 17$	$-23 \le h \le 23$, $-18 \le k \le 17$, $-16 \le l \le 24$
Reflections collected/unique	8292/5266 [$R_{int} = 0.0162$]	8159/5180 [$R_{int} = 0.0167$]	31324/10305 [$R_{int} = 0.0287$]
Data/restraints/parameters	5266/0/415	5180/0/406	10305/2/829
Goodness-of-fit on F^2	1.074	1.032	1.037
Final R indices [$I > 2\sigma(I)$]	$R_1 = 0.0261$, $wR_2 = 0.0621$	$R_1 = 0.0222$, $wR_2 = 0.0512$	$R_1 = 0.0238$, $wR_2 = 0.0538$
R indices (all data)	$R_1 = 0.0316$, $wR_2 = 0.0635$	$R_1 = 0.0277$, $wR_2 = 0.0525$	$R_1 = 0.0331$, $wR_2 = 0.0563$
Largest diff. peak and hole (e Å^{-3})	0.465 and −0.527	0.307 and −0.370	0.508 and −0.470

Crystallographic data and experimental details for structural analyses are summarized in table 1. Selected bond lengths and angles are listed in tables 2–4 for **1**, **2** and **3**, respectively.

3. Results and discussion

3.1. *The IR spectra of the complexes*

IR spectra of the complexes recorded from 3500 to 350 cm^{-1} are very similar, indicating similar coordination of the ligands to the central ions. The infrared spectra of the complexes, listed in table 5, were compared to that of the organic ligands.

The characteristic absorption of fluorobenzoic acid $\nu_{C=O}$(–COOH) and δ_{O-H} (–COOH) completely disappears in the spectra of the complexes. However, the peak arising from asymmetric and symmetric vibrations of the COO^- group occur at 1603, 1603, 1612 cm^{-1} and 1414, 1421, 1410 cm^{-1} for **1**, **2**, **3**, respectively, indicating that the carboxyl groups are bonded to the central ions, which was confirmed by X-ray diffraction analysis. In addition, the absorption of $\nu_{C=N}$ (1560 cm^{-1}) of 1,10-phenanthroline shifts to lower wavenumber 1514, 1543 and 1545 cm^{-1}, respectively, indicating that the nitrogen atoms of 1,10-phenanthroline coordinate to the central ions.

Table 2. Selected bond lengths (Å) and angles (°) for [Eu(*p*-FBA)$_3$(phen)(H$_2$O)]$_2$ (**1**).

Eu(1)–O(5)	2.332(2)	Eu(1)–O(3)	2.388(2)
Eu(1)–O(1)	2.365(3)	Eu(1)–O(7)	2.430(2)
Eu(1)–O(4)#1	2.378(2)	Eu(1)–N(1)	2.598(3)
Eu(1)–O(6)#1	2.401(2)	Eu(1)–N(2)	2.642(3)
O(5)–Eu(1)–O(1)	87.20(9)	O(5)–Eu(1)–O(3)	72.72(7)
O(5)–Eu(1)–O(4)#1	77.43(8)	O(5)–Eu(1)–O(7)	144.31(8)
O(5)–Eu(1)–O(6)#1	122.66(8)	O(5)–Eu(1)–N(2)	79.23(9)
O(5)–Eu(1)–N(1)	138.09(9)	O(3)–Eu(1)–O(6)#1	85.98(8)
O(3)–Eu(1)–O(7)	76.11(7)	O(3)–Eu(1)–N(1)	149.00(9)
O(3)–Eu(1)–N(2)	140.6(1)	O(1)–Eu(1)–O(3)	83.27(9)
O(4)#1–Eu(1)–O(3)	126.69(8)	O(1)–Eu(1)–N(1)	93.4(1)
O(1)–Eu(1)–O(4)#1	138.25(8)	O(1)–Eu(1)–O(7)	72.17(8)
O(1)–Eu(1)–O(6)#1	143.25(8)	O(1)–Eu(1)–N(2)	68.0(1)
O(7)–Eu(1)–N(2)	116.94(9)	O(4)#1–Eu(1)–O(7)	136.72(8)
O(7)–Eu(1)–N(1)	73.57(9)	O(6)#1–Eu(1)–O(7)	71.15(8)
O(4)#1–Eu(1)–N(1)	74.53(9)	O(4)#1–Eu(1)–O(6)#1	74.39(8)
O(4)#1–Eu(1)–N(2)	71.07(9)	O(6)#1–Eu(1)–N(1)	78.4(1)
O(6)#1–Eu(1)–N(2)	133.1(1)	N(1)–Eu(1)–N(2)	62.6(1)

Symmetry transformations used to generate equivalent atoms: #1: $-x+1$, $-y+1$, $-z+1$.

Table 3. Selected bond lengths (Å) and angles (°) for [Tb(*p*-FBA)$_3$phen]$_2$ (**2**).

Tb(1)–O(2)#1	2.283(2)	Tb(1)–O(6)	2.353(2)
Tb(1)–O(3)#1	2.331(2)	Tb(1)–O(5)	2.512(2)
Tb(1)–O(4)	2.340(2)	Tb(1)–N(1)	2.564(2)
Tb(1)–O(1)	2.344(2)	Tb(1)–N(2)	2.632(2)
O(2)#1–Tb(1)–O(3)#1	79.14(8)	O(2)#1–Tb(1)–N(1)	85.73(8)
O(2)#1–Tb(1)–O(4)	76.10(8)	O(2)#1–Tb(1)–O(1)	124.79(8)
O(2)#1–Tb(1)–O(6)	132.35(8)	O(2)#1–Tb(1)–O(5)	80.17(8)
O(2)#1–Tb(1)–N(2)	139.50(8)	O(3)#1–Tb(1)–O(4)	126.51(7)
O(3)#1–Tb(1)–N(1)	80.58(8)	O(3)#1–Tb(1)–N(2)	71.07(8)
O(3)#1–Tb(1)–O(1)	79.51(8)	O(3)#1–Tb(1)–O(6)	146.06(7)
O(3)#1–Tb(1)–O(5)	145.42(8)	O(4)–Tb(1)–N(1)	142.20(8)
O(4)–Tb(1)–N(2)	144.17(8)	O(4)–Tb(1)–O(1)	77.18(7)
O(4)–Tb(1)–O(6)	80.13(7)	O(4)–Tb(1)–O(5)	73.87(7)
O(1)–Tb(1)–N(1)	138.85(7)	O(1)–Tb(1)–N(2)	76.35(7)
O(1)–Tb(1)–O(6)	88.19(8)	O(1)–Tb(1)–O(5)	135.00(8)
O(6)–Tb(1)–N(2)	75.33(7)	O(6)–Tb(1)–N(1)	88.67(8)
O(6)–Tb(1)–O(5)	53.60(7)	O(5)–Tb(1)–N(1)	70.50(7)
O(5)–Tb(1)–N(2)	109.96(7)	N(1)–Tb(1)–N(2)	63.19(7)

Symmetry transformations used to generate equivalent atoms: #1: $-x+1$, $-y$, $-z+1$.

3.2. *Structural description of the title complexes*

3.2.1. Crystal structure of 1. The molecular structure and atomic numbering of [Eu(*p*-FBA)$_3$(phen)(H$_2$O)]$_2$ (**1**) are shown in figure 1. The two Eu(III) ions are linked together by four *p*-FBA groups through their bidentate bridging modes, forming a dimeric unit with a crystallographic inversion center. Each Eu(III) is coordinated to eight atoms, of which four oxygen atoms are from the bridging carboxylates, one oxygen from a monodentate carboxylate, one oxygen of H$_2$O and two nitrogen atoms from 1,10-phenanthroline. The coordination polyhedron of Eu(III) is a distorted square antiprism. Coordinated water in the inner coordination surroundings is rare for ternary europium carboxylate complexes, only found in

Table 4. Selected bond lengths (Å) and angles (°) for $[Tb(o\text{-}FBA)_3phen]_2$ (**3**).

Tb(1)–O(1)	2.316(2)	Tb(2)–O(10)	2.291(2)
Tb(1)–O(3)	2.322(2)	Tb(2)–O(7)#2	2.305(2)
Tb(1)–O(2)#1	2.339(2)	Tb(2)–O(9)#2	2.333(2)
Tb(1)–O(4)#1	2.371(2)	Tb(2)–O(8)	2.342(2)
Tb(1)–O(5)	2.401(2)	Tb(2)–O(12)	2.387(2)
Tb(1)–O(6)	2.473(2)	Tb(2)–O(11)	2.504(2)
Tb(1)–N(2)	2.538(2)	Tb(2)–N(3)	2.554(3)
Tb(1)–N(1)	2.609(3)	Tb(2)–N(4)	2.630(3)
O(1)–Tb(1)–O(3)	78.42(9)	O(10)–Tb(2)–O(7)#2	75.09(10)
O(1)–Tb(1)–O(2)#1	131.34(8)	O(10)–Tb(2)–O(9)#2	125.77(9)
O(1)–Tb(1)–O(4)#1	76.05(8)	O(10)–Tb(2)–O(8)	80.56(9)
O(1)–Tb(1)–O(5)	128.68(8)	O(10)–Tb(2)–O(12)	83.86(9)
O(1)–Tb(1)–O(6)	75.27(7)	O(10)–Tb(2)–O(11)	75.24(9)
O(1)–Tb(1)–N(2)	81.44(8)	O(10)–Tb(2)–N(3)	141.99(10)
O(1)–Tb(1)–N(1)	135.91(8)	O(10)–Tb(2)–N(4)	145.48(9)
O(3)–Tb(1)–O(2)#1	73.23(8)	O(7)#2–Tb(2)–O(9)#2	81.66(9)
O(3)–Tb(1)–O(4)#1	126.77(10)	O(7)#2–Tb(2)–O(8)	126.64(8)
O(3)–Tb(1)–O(6)	76.81(8)	O(7)#2–Tb(2)–O(12)	88.97(8)
O(3)–Tb(1)–O(5)	89.50(10)	O(7)#2–Tb(2)–O(11)	133.89(8)
O(3)–Tb(1)–N(2)	145.00(8)	O(7)#2–Tb(2)–N(3)	140.84(9)
O(3)–Tb(1)–N(1)	144.98(8)	O(7)#2–Tb(2)–N(4)	78.08(9)
O(2)#1–Tb(1)–O(4)#1	90.31(9)	O(9)#2–Tb(2)–O(8)	75.40(9)
O(2)#1–Tb(1)–O(5)	90.08(8)	O(9)#2–Tb(2)–O(12)	144.37(9)
O(2)#1–Tb(1)–O(6)	132.46(8)	O(9)#2–Tb(2)–O(11)	144.40(9)
O(2)#1–Tb(1)–N(1)	76.17(8)	O(9)#2–Tb(2)–N(3)	81.15(9)
O(2)#1–Tb(1)–N(2)	139.81(8)	O(9)#2–Tb(2)–N(4)	70.17(9)
O(4)#1–Tb(1)–O(6)	137.20(8)	O(8)–Tb(2)–O(12)	134.72(8)
O(4)#1–Tb(1)–O(5)	141.96(8)	O(8)–Tb(2)–O(11)	81.50(8)
O(4)#1–Tb(1)–N(2)	74.36(9)	O(8)–Tb(2)–N(3)]	81.93(8)
O(4)#1–Tb(1)–N(1)	69.40(8)	O(8)–Tb(2)–N(4)	133.56(8)
O(5)–Tb(1)–O(6)	53.41(7)	O(12)–Tb(2)–O(11)	53.40(8)
O(5)–Tb(1)–N(2)	81.12(8)	O(12)–Tb(2)–N(3)	84.97(9)
O(5)–Tb(1)–N(1)	73.81(8)	O(12)–Tb(2)–N(4)	74.28(8)
O(6)–Tb(1)–N(2)	70.51(8)	O(11)–Tb(2)–N(3)	68.96(9)
O(6)–Tb(1)–N(1)	113.62(8)	O(11)–Tb(2)–N(4)	110.10(8)
N(2)–Tb(1)–N(1)	63.70(8)	N(3)–Tb(2)–N(4)	63.03(9)

Symmetry transformations used to generate equivalent atoms: #1: $-x+1, -y+1, -z+2$; #2: $-x, -y, -z$.

Table 5. IR spectral data of ligands and complexes (cm^{-1}).

	–COOH		–COO^-			
Compound	$\nu_{C=O}$	δ_{O-H}	ν_{as}	ν_s	$\nu_{C=N}$	ν_{O-H}
phen					1560	3402
p-FBA	1682	924				
o-FBA	1693	920				
$[Eu(p\text{-}FBA)_3phen(H_2O)]_2$			1603	1414	1514	3474
$[Tb(p\text{-}FBA)_3phen]_2$			1603	1421	1543	
$[Tb(o\text{-}FBA)_3phen]_2$			1612	1410	1545	

$[Eu(m\text{-}BrBA)_3(phen)(H_2O)]_2$ [26] The majority of analogues display an anhydrous dimer, such as in $[Eu(BA)_3(phen)]_2$ [27], and $[Eu(BA)_3(bipy)]_2$ [28]. The uncommon coordination may arise from the steric effect of the halogen substituent atom on the benzene, while the terminal carboxylate becomes monodentate.

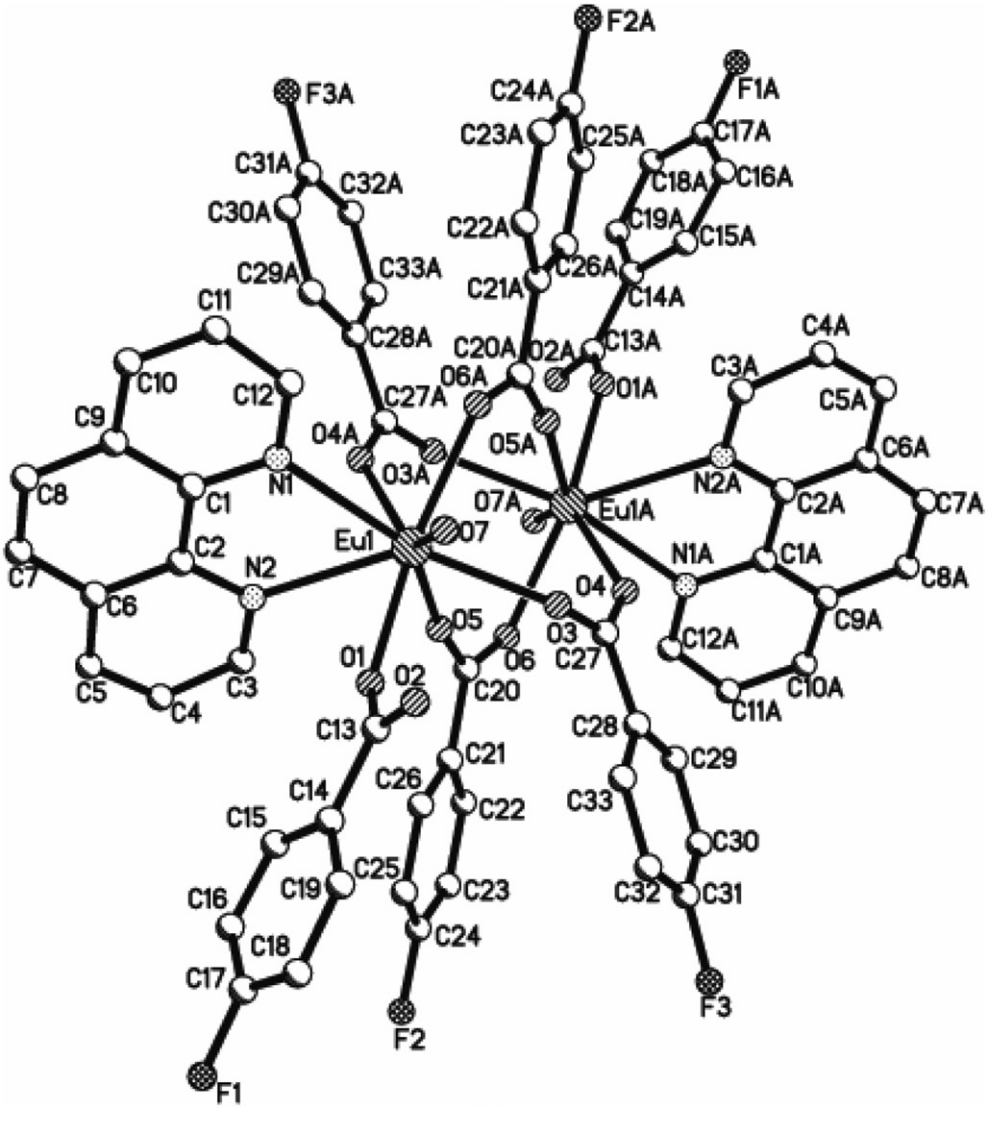

Figure 1. ORTEP drawing of **1**.

Selected bond distances and angles for [Eu(*p*-FBA)$_3$(phen)(H$_2$O)]$_2$ (**1**) are listed in table 2. The O–Eu–O (bridging carboxylate oxygen) bond angles lie in the range of 72.72(7)–126.69(8)°, the N–Eu–N bond angles are 62.6(1)°. The distance between Eu(III) ions is 4.333 Å. The Eu–O lengths are in a range of 2.332(2)–2.430(2) Å, with the bond formed by H$_2$O the longest (Eu(1)–O(7) = 2.430(2) Å). The average Eu–O bond length is 2.382(2) Å, slightly shorter than that of [Eu(*p*-ClBA)$_3$phen]$_2$ (2.392 Å) [29]. The average Eu–N bond length (2.620(3) Å) is also shorter than in [Eu(*p*-ClBA)$_3$phen]$_2$ (2.631 Å), indicating that the Eu–O and Eu–N bonds of **1** are both stronger than those in [Eu(*p*-ClBA)$_3$phen]$_2$, perhaps from electronic effects of the fluorine atoms on the benzene. Intermolecular hydrogen bonds were formed among the coordinated water

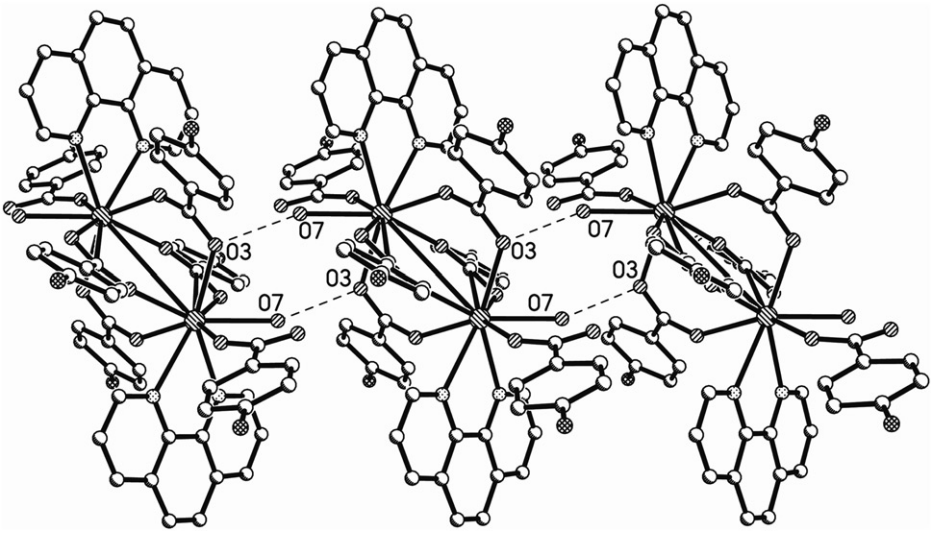

Figure 2. 1-D chain for **1** with hydrogen bonds.

molecules and the bridging carboxylate oxygen atoms [O7 $\cdots$ O3[$-x+2$, $-y+1$, $-z+1$] = 2.820 Å] along the *a*-axis, generating an infinite 1-D chain, as shown in figure 2.

3.2.2. Crystal structure of complex 2. The molecular structure and atomic numbering of [Tb(*p*-FBA)$_3$phen]$_2$ (**2**) are shown in figure 3. The two Tb(III) ions are linked together by four bidentate bridging *p*-fluorobenzoates, forming a dimer with a crystallographic inversion center. Each Tb(III) is coordinated to eight atoms, four oxygens from the bridging carboxylates, two oxygens from the bidentate chelating carboxylate and two nitrogens from a 1,10-phenanthroline. Similar to **1**, the central Tb(III) also has a distorted square antiprism geometry. There is no H_2O coordinated to Tb(III), different from **1**.

Selected bond distances and angles for **2** are listed in table 3. The distance between two Tb(III) ions is 4.281 Å, slightly shorter than that between two Eu(III) ions in **1**. The O–Tb–O (bridging carboxylate oxygen) bond angles are in the range of 76.10(8)–126.51(7)° and the N–Tb–N bond angle is 63.19(7)°. The Tb–O bond lengths are in a range of 2.283(2)–2.512(2) Å, with Tb–O bonds formed by the bidentate chelating carboxylate oxygen slightly longer (2.512(2) and 2.353(2) Å) than those formed by the bridging carboxylate (2.283(2)–2.344(2) Å). The average Tb–O bond length is 2.361(2) Å in **2**, shorter than the average Eu–O bond length in **1**. The average Tb–N bond length (2.598 Å) is also shorter than the average Eu–N bond length in **1**, arising from the radii of the central ions. Eu(III) is slightly larger than Tb(III), so the H_2O coordinates to Eu(III) in **1**, but cannot coordinate Tb(III) in **2**.

3.2.3. Crystal structure of complex 3. Different from **1** and **2**, **3** contains two independent dimeric molecules [Tb(*o*-FBA)$_3$(phen)]$_2$, noted as [Tb-1] and

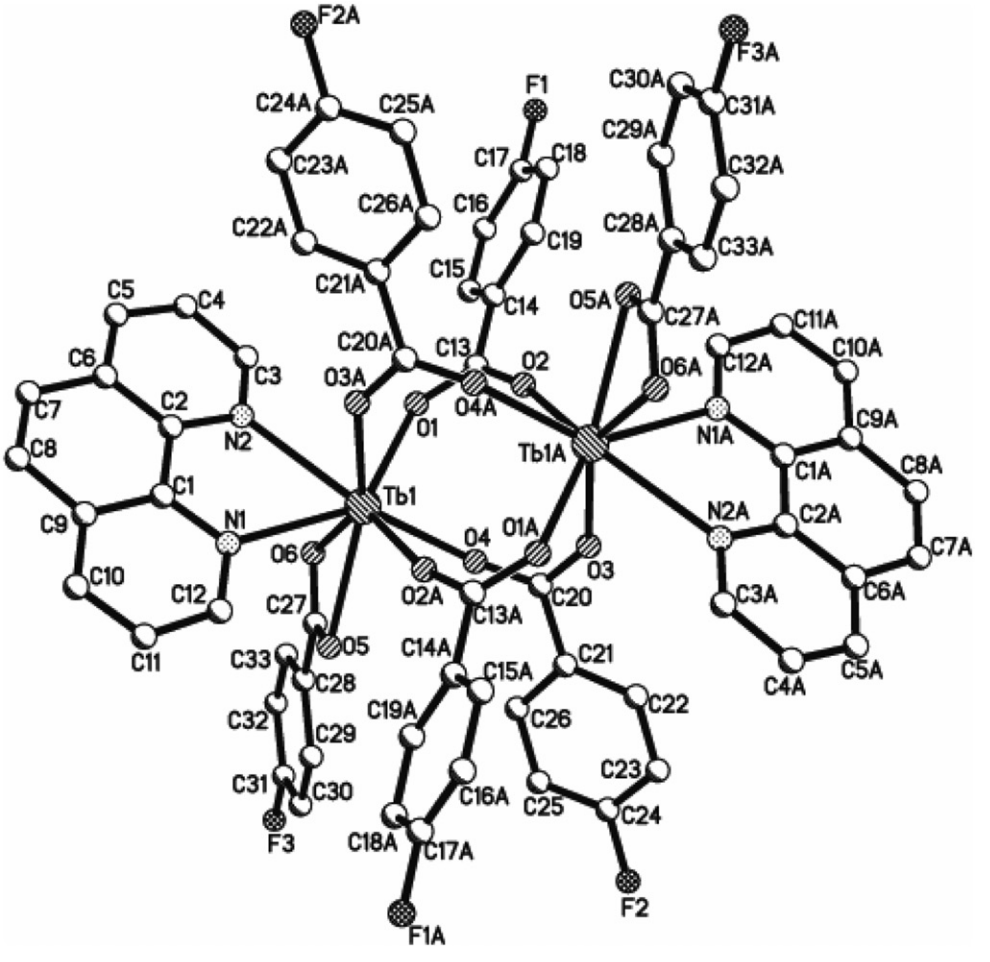

Figure 3. ORTEP drawing of **2**.

[Tb-2], respectively. Their structures are shown in figure 4. (a and b for [Tb-1] and [Tb-2], respectively). Selected bond lengths and angles are listed in table 4. [Tb-1] and [Tb-2] are identical in composition with similar structures. In each molecule, two Tb(III) ions are linked by four bidentate bridging carboxylate groups forming a dimer with a crystallographic inversion center. The intramolecular distances between two Tb(III) ions are 4.129 Å for [Tb-1], and 4.245 Å for [Tb-2]. Each Tb(III) ion is an eight-coordinate distorted square antiprism, with four coordination sites occupied by the oxygen atoms from the bridging carboxylates, two by oxygens from the bidentate chelating carboxylate, and the remaining positions occupied by two nitrogens from a 1,10-phenanthroline.

Disorder is observed for the fluorine atoms on the terminal *o*-fluorobenzoate ligands. The five-member chelate ring containing two nitrogen atoms and the terbium ion are coplanar to the 1,10-phenanthroline plane. For [Tb-1], the Tb–O bond lengths vary from 2.316(2) to 2.473(2) Å, and the average bond length is 2.370(2) Å, slightly longer

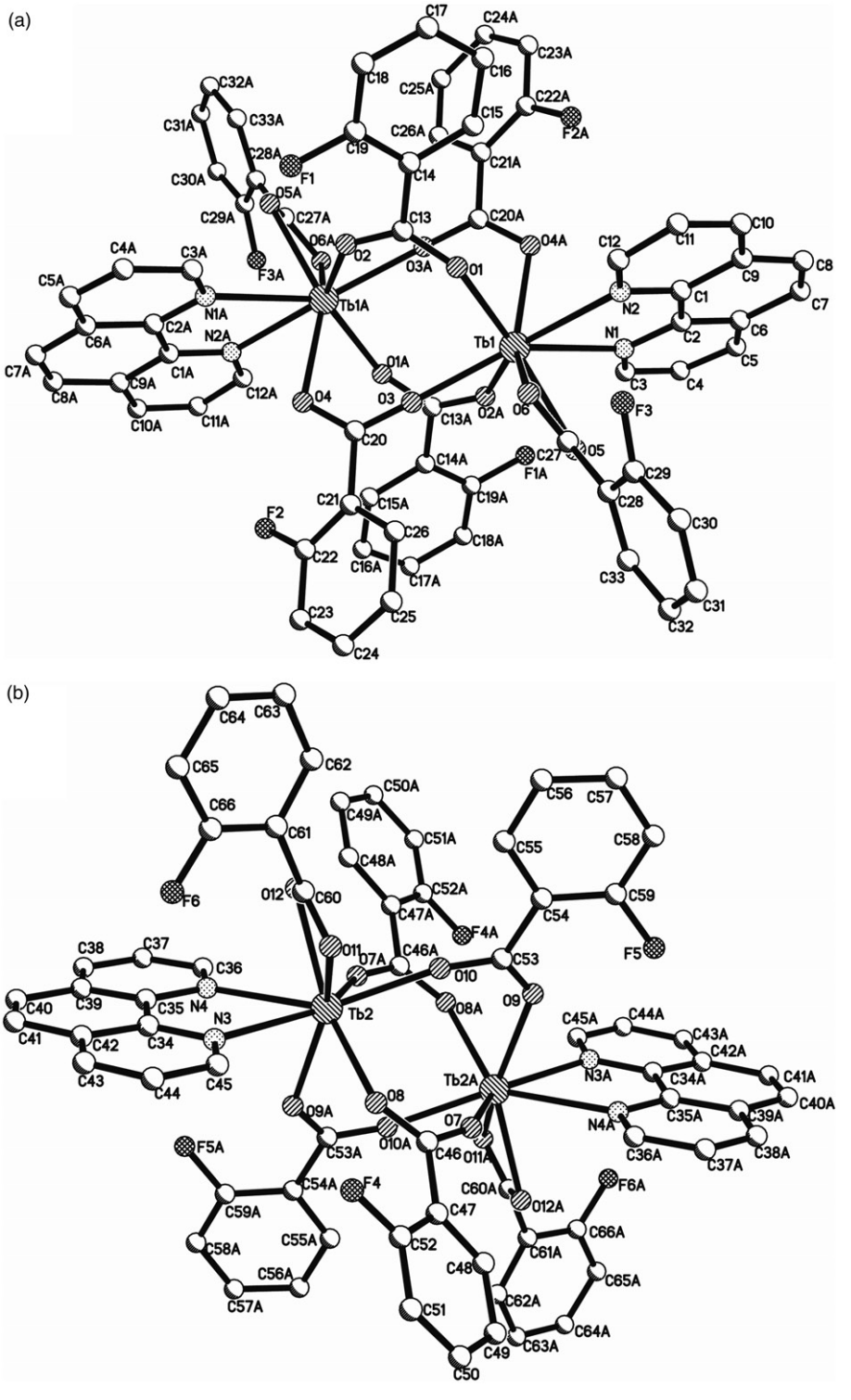

Figure 4. ORTEP drawing of **3**: (a) [Tb-1]; (b) [Tb-2].

than that of [Tb(*p*-FBA)$_3$phen]$_2$ (2.361(2) Å). The average Tb–N bond length is 2.574(2) Å, shorter than that of [Tb(*p*-FBA)$_3$phen]$_2$ (2.598 Å) indicating that the interaction between Tb(III) and oxygen in [Tb-1] is weaker than that of [Tb(*p*-FBA)$_3$phen]$_2$ (**2**), but the interaction between Tb(III) and nitrogen atoms in [Tb-1] is stronger than that of [Tb(*p*-FBA)$_3$phen]$_2$ (**2**). In [Tb-2], the Tb–O bond length is in a range of 2.291(2)–2.504(2) Å with the mean bond length 2.360(2) Å, shorter than in [Tb-1]. The average Tb–N bond length is 2.592 Å, longer than in [Tb-1], indicating that the interaction between Tb(III) ions and oxygens in [Tb-2] is stronger than in [Tb-1], but the corresponding interactions of Tb(III) and nitrogen atoms is weaker than in [Tb-1].

3.3. *Luminescence properties*

All excitation and luminescence of powder complexes were performed under identical conditions and instrumental parameters at room temperature (as shown in figures 5 and 6). The excitation of all three complexes were effected in a range of 200–400 nm. Fluorescence was observed in a range of 400–700 nm by selective excitation at 328 nm. All of these ternary complexes show intense luminescent properties at room temperature.

The emission spectrum for **1** is composed of the characteristic emission peaks of Eu(III) arising from transitions $^5D_0 \rightarrow {}^7F_0$ (579 nm), $^5D_0 \rightarrow {}^7F_1$ (590, 595 nm), $^5D_0 \rightarrow {}^7F_2$ (612, 618, 619, 620 nm), respectively. The intensity of the emission band arising from $^5D_0 \rightarrow {}^7F_2$ is the most intense, similar to complexes in the literature [26, 29, 30].

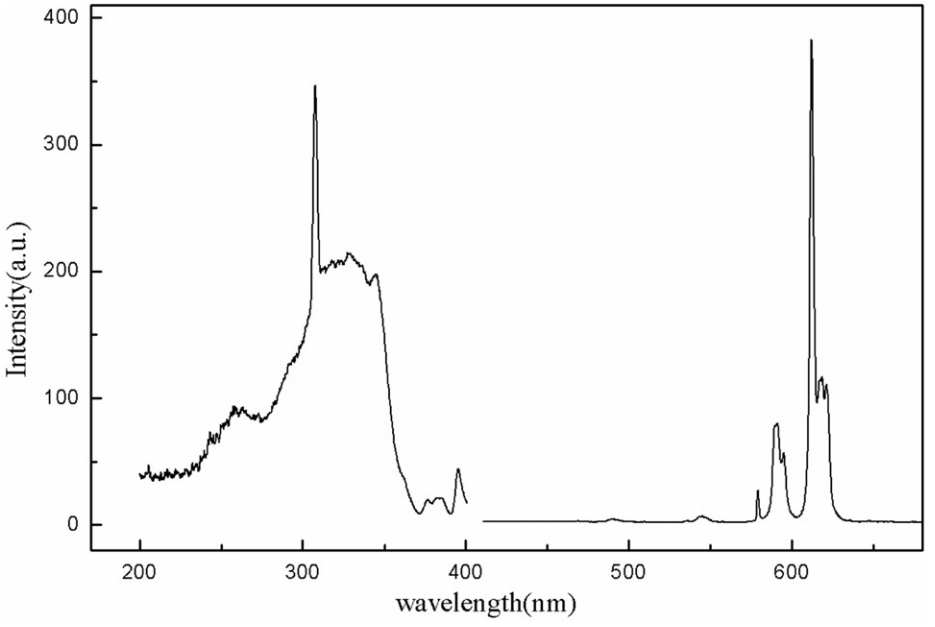

Figure 5. Excitation spectra and luminescence spectra ($\lambda_{ex} = 328$ nm) of **1**.

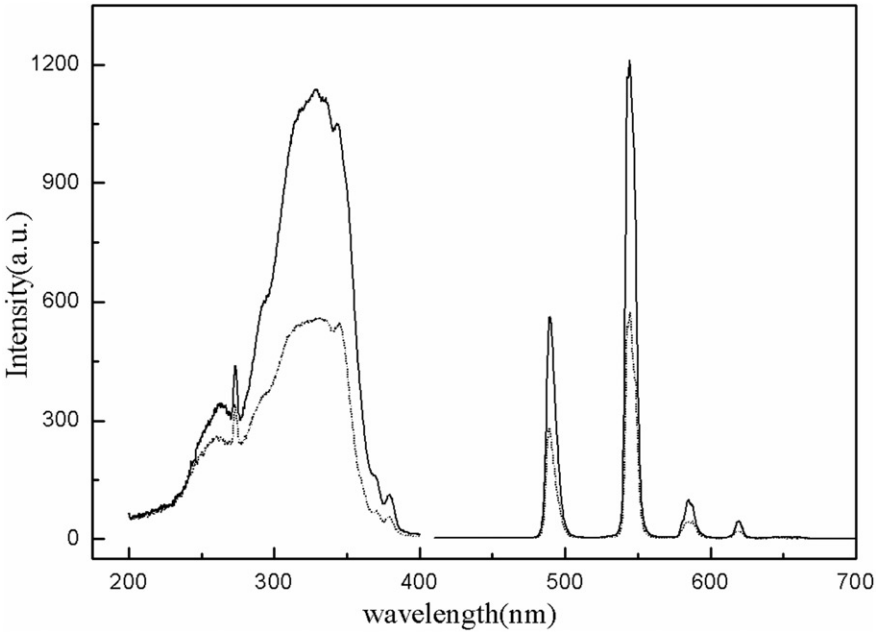

Figure 6. Excitation spectra and luminescence spectra ($\lambda_{ex} = 328$ nm) of **2** and **3**. · · ·: [Tb(*p*-FBA)$_3$phen]$_2$ (**2**); —: [Tb(*o*-FBA)$_3$phen]$_2$ (**3**).

Compared the emission spectra of **2** and **3** (figure 6), no distinct change is observed in their profiles, with four characteristic emission peaks of Tb(III): $^5D_4 \rightarrow {}^7F_6$ (489 nm), $^5D_4 \rightarrow {}^7F_5$ (545 nm), $^5D_4 \rightarrow {}^7F_4$ (587 nm), $^5D_4 \rightarrow {}^7F_3$ (620 nm), respectively. The most intense emission band arises from the $^5D_4 \rightarrow {}^7F_5$ transition. However, the emission intensity of **3** is larger than that of **2**, indicating that *o*-fluorobenzoate is a more appropriate ligand for luminescent ternary Tb(III) complexes than *p*-fluorobenzoate. This is related to the electronic effect of fluorine at different positions of benzene.

3.4. *Thermal decomposition*

The TG and DTG curves of **1**–**3** are shown in figure 7. [Eu(*p*-FBA)$_3$(phen)(H$_2$O)]$_2$ (**1**) decomposed via intermediates to give europium oxide. It begins to decompose at 290°C and its decomposition ends at about 896°C. The TG degradation reveals three decomposition stages, consistent with the DTG curve. There are maximum weight loss rates at 357 and 586°C in the DTG curve. Compared with [Eu(*m*-ClBA)$_3$phen]$_2$ [30] and [Eu(*m*-BrBA)$_3$(H$_2$O)phen]$_2$ [26], [Eu(*m*-ClBA)$_3$phen]$_2$ begins to decompose at 244°C and [Eu(*m*-BrBA)$_3$(H$_2$O)phen]$_2$ begins to decompose at 264°C. So [Eu(*p*-FBA)$_3$(phen)(H$_2$O)]$_2$ is more stable than [Eu(*m*-ClBA)$_3$phen]$_2$ and [Eu(*m*-BrBA)$_3$(H$_2$O)phen]$_2$.

For **1**, the first degradation stage starts from 290 to 446°C with a mass loss of 23.29%, corresponding to loss of 2 mol $C_{12}H_8N_2$ and 2 mol H_2O (theoretical loss is 25.83 wt%). This can be explained by the bond distances (table 2): Eu–N distance is longer than any other bond distance, so the bonds are less stable and easily broken.

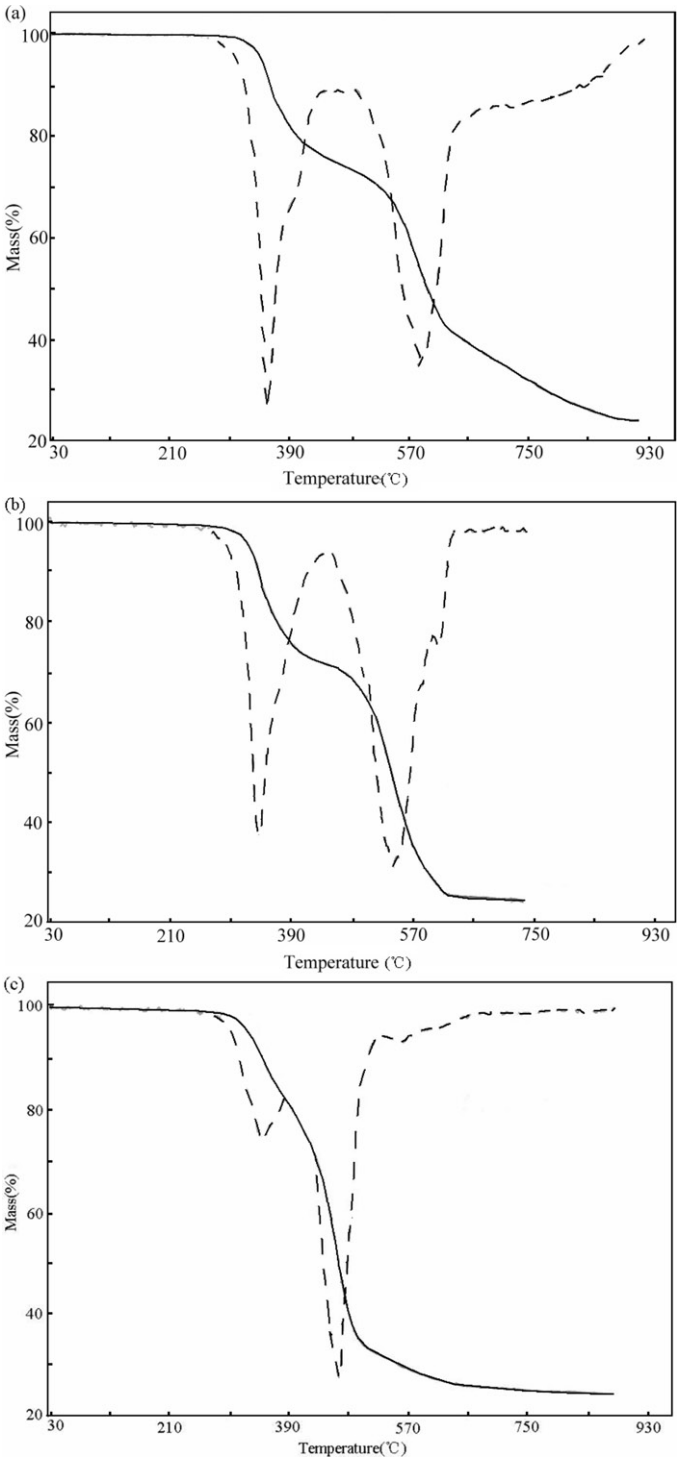

Figure 7. Thermogravimetric curves (DTG and TG) for **1**–**3**. (a) [Eu(*p*-FBA)$_3$phen(H$_2$O)]$_2$ (**1**); (b) [Tb(*p*-FBA)$_3$phen]$_2$ (**2**); (c) [Tb(*o*-FBA)$_3$phen]$_2$ (**3**).

The Eu(1)–O(7) bond is longer than other Eu–O bonds but shorter than Eu–N bonds, so it is comparatively easily broken, too. The second degradation stage is in the range of 446–655°C with mass loss of 36.49%, corresponding to the loss of [4 mol (p-FC_6H_4COO)] (theoretical loss is 36.25 wt%). The third degradation stage is in the range of 655–896°C with mass loss of 15.33%, which [2 mol(p-FC_6H_4COO)–3 molO] removed with theoretical loss of 15.00 wt%. 1,10-Phenanthroline-tris(p-fluorobenzoate)–H_2O europium(III) was completely degraded into Eu_2O_3 with a total loss of 75.11 wt% (theoretical loss is 77.07 wt%). The thermal decomposition of [Eu(p-FBA)$_3$(phen)(H_2O)]$_2$ can be described as follows:

$$\left[\mathrm{Eu}(p-\mathrm{FBA})_3(\mathrm{phen})(\mathrm{H_2O})\right]_2 \rightarrow \mathrm{Eu_2}(p-\mathrm{FBA})_6 \rightarrow \mathrm{Eu_2}(p-\mathrm{FBA})_2 \rightarrow \mathrm{Eu_2O_3}$$

The decomposition processes of **2** and **3** are similar to **1**, but with two decomposition stages. The first degradation stage of **2** is in the range 263–443°C, corresponding to the loss of 2 mol $C_{12}H_8N_2$. Complex **3** begins to decompose at 285°C, slightly more stable than **2.** Their decomposition processes can be described as follows:

$$\left[\mathrm{Tb}(p-\mathrm{FBA})_3\mathrm{phen}\right]_2 \rightarrow \mathrm{Tb_2}(p-\mathrm{FBA})_6 \rightarrow \frac{1}{2}\mathrm{Tb_4O_7}$$

$$\left[\mathrm{Tb}(o-\mathrm{FBA})_3\mathrm{phen}\right]_2 \rightarrow \mathrm{Tb_2}(o-\mathrm{FBA})_6 \rightarrow \frac{1}{2}\mathrm{Tb_4O_7}$$

In conclusion, three dimeric rare-earth complexes [Eu(p-FBA)$_3$(phen)(H_2O)]$_2$ (**1**), [Tb(p-FBA)$_3$phen]$_2$ (**2**), and [Tb(o-FBA)$_3$phen]$_2$ (**3**) have been synthesized. Complex **1** shows bright red luminescence, while **2** and **3** show green luminescence under UV light at room temperature. Complex **3** is a more effective luminescence complex than **2**. The thermal analysis indicates that they are all quite stable.

Supplementary data

CCDC-608068, 608069, 608070 contain the supplementary crystallographic data for this article. These data can be obtained free of charge via www.ccdc.cam.ac.uk/conts/retrieving.html (or from the Cambridge crystallographic Data Centre, 12, Union Road, Cambridge CB2 1EZ, UK; Fax: +44 1223 336033).

Acknowledgements

This work was supported by the Natural Science Foundation of Hebei Province (No. 203148) and Hebei Education Department (No. 2006125), P.R. China.

References

[1] Y.B. Wang, X.J. Zheng, W.J. Zhuang, L.P. Jin. *Eur. J. Inorg. Chem.*, 3572 (2003).
[2] C.B. Liu, C.Y. Sun, L.P. Jin, S.Z. Lu. *New. J. Chem.*, **28**, 1019 (2004).
[3] C.Y. Sun, X.J. Zheng, L.P. Jin. *Z. Anorg. Allg. Chem.*, **630**, 1342 (2004).
[4] A.W.H. Lam, W.T. Wong, S. Gao, G.H. Wen, X.X. Zhang. *Eur. J. Inorg. Chem.*, 149 (2003).
[5] B. Barja, P. Aramendia, R. Baggio, M.T. Garland, O. Peña, M. Perec. *Inorg. Chim. Acta*, **355**, 183 (2003).
[6] Y.B. Wang, X.J. Zheng, W.J. Zhuang, L.P. Jin. *Eur. J. Inorg. Chem.*, 1355 (2003).

[7] M.C. Yin, L.J. Yuan, C.C. Ai, C.W. Wang, E.T. Yuan, J.T. Sun. *Polyhedron*, **23**, 529 (2004).
[8] J.G. Mao, H.J. Zhang, J.Z. Ni, S.B. Wang, T.C.W. Mak. *Polyhedron*, **17**, 3999 (1998).
[9] X. Li, Z.Y. Zhang, Y.Q. Zou. *Eur. J. Inorg. Chem.*, 2909 (2005).
[10] L. Oyang, H.L. Sun, X.Y. Wang, J.R. Li, D.B. Nie, W.F. Fu, S. Gao, K.B. Yu. *J. Mol. Struct.*, **740**, 175 (2005).
[11] G.H. Cui, J.R. Li, R.H. Zhang, X.H. Bu. *J. Mol. Struct.*, **740**, 187 (2005).
[12] B. Yan, Y.S. Song, Z.X. Chen. *J. Mol. Struct.*, **694**, 115 (2004).
[13] S.V. Eliseeva, O.V. Mirzov, S.I. Troyanov, A.G. Vitukhnovsky, N.P. Kuzmina. *J. Alloy. Compd.*, **374**, 293 (2004).
[14] M.C. Yin, C.C. Ai, L.J. Yuan, C.W. Wang, J.T. Sun. *J. Mol. Struct.*, **691**, 33 (2004).
[15] L.J. Yuan, M.C. Yin, E.T. Yuan, J.T. Sun, K.L. Zhang. *Inorg. Chim. Acta*, **357**, 89 (2004).
[16] S.P. Yang, H. Yang, X.B. Yu, Z.M. Wang. *J. Mol. Struct.*, **659**, 97 (2003).
[17] J.C.G. Bünzli. In *Lanthanide Probes in life, Chemical and Earth Science, Theory and Practice*, J.C.G. Bünzli, G.R. Choppin (Eds), Chap. 7, Elsevier, Amsterdam (1989).
[18] M. Elbanowski, B. Makowska. *J. Photochem. Photobio. A: Chem.*, **99**, 85 (1996).
[19] B.H. Lee, K.H. Chung, H.S. Shin, Y.J. Park, H. Moon. *J. Colloid Interf. Sci.*, **188**, 439 (1997).
[20] B. Yan, H.J. Zhang, S.B. Wang, J.Z. Ni. *J. Photochem. Photobio. A: Chem. I*, **12**, 231 (1998).
[21] B.S. Panigrahi. *Spectrochim. Acta A*, **56**, 1337 (2000).
[22] W.W. Qin, Y.L. Zhang, W.S. Liu, M.Y. Tan. *Spectrochim. Acta A*, **59**, 3085 (2003).
[23] L.P. Jin, M.Z. Wang, G.L. Cai, S.X. Liu, J.L. Huang, R.F. Wang. *Sci. China (Ser. B)*, **38**, 1 (1995).
[24] R.F. Wang, L.P. Jin, M.Z. Wang, S.H. Huang, X.T. Chen. *Acta Chim. Sin.*, **53**, 39 (1995).
[25] L.P. Jin, R.F. Wang, L.S. Li, S.Z. Lu, S.H. Huang. *Polyhedron*, **18**, 487 (1998).
[26] R.F. Wang, S.P. Wang, J.J. Zhang. *J. Mol. Struct.*, **648**, 151 (2003).
[27] Y. Zhang, L.P. Jin, S.Z. Lv. *J. Chinese Rare Earth Soc.*, **16**, 5 (1998).
[28] Y. Zhang, L.P. Jin, S.Z. Lv. *Chinese J. Inorg. Chem.*, **13**, 280 (1997).
[29] L.P. Jin, R.F. Wang, L.S. Li, S.Z. Lu. *J. Rare Earth*, **14**, 161 (1996).
[30] R.F. Wang, S.P. Wang, J.J. Zhang. *J. Rare Earth*, **22**, 816 (2004).
[31] G.M. Sheldrick. *SHELXS-97: Program for the Solution of Crystal Structures*, University of Göttingen, Germany (1997).
[32] G.M. Sheldrick. *SHELXL-97: Program for the Refinement of Crystal Structures*, University of Göttingen, Germany (1997).